

The following resources related to this article are available online at www.sciencemag.org (this information is current as of November 9, 2009):

Updated information and services, including high-resolution figures, can be found in the online version of this article at:

<http://www.sciencemag.org/cgi/content/full/326/5952/585>

Supporting Online Material can be found at:

<http://www.sciencemag.org/cgi/content/full/1179052/DC1>

A list of selected additional articles on the Science Web sites **related to this article** can be found at:

<http://www.sciencemag.org/cgi/content/full/326/5952/585#related-content>

This article **cites 20 articles**, 7 of which can be accessed for free:

<http://www.sciencemag.org/cgi/content/full/326/5952/585#otherarticles>

This article has been **cited by** 1 articles hosted by HighWire Press; see:

<http://www.sciencemag.org/cgi/content/full/326/5952/585#otherarticles>

This article appears in the following **subject collections**:

Virology

<http://www.sciencemag.org/cgi/collection/virology>

Information about obtaining **reprints** of this article or about obtaining **permission to reproduce this article** in whole or in part can be found at:

<http://www.sciencemag.org/about/permissions.dtl>

the pathophysiology of chytridiomycosis appears to be disruption to the osmoregulatory functioning of the skin and consequent osmotic imbalance that leads to cardiac standstill.

To test whether treating electrolyte abnormalities would reduce the clinical signs of disease, we administered an oral electrolyte supplement to *L. caerulea* in the terminal stages of infection, when they lost the righting reflex and could no longer correct their body positions (26). Frogs under treatment recovered a normal posture and became more active; one individual recovered sufficiently to climb out of the water onto the container walls, and two individuals were able to jump to avoid capture. These signs of recovery were not observed in any untreated frogs. In addition, treated frogs lived >20 hours longer than untreated frogs [mean time after treatment \pm SEM: treated frogs ($N = 9$), 32 ± 2.8 hours; control frogs ($N = 6$), 10.7 ± 2.2 hours; Student's *t* test, $P < 0.001$]. All treated frogs continued to shed skin and ultimately died from the infection, as expected. It is unlikely that electrolyte treatment could prevent death unless the epidermal damage caused by *Bd* is reversed. Although amphibians can generally tolerate greater electrolyte fluctuations than other terrestrial vertebrates (18), we suggest that depletion of electrolytes, especially potassium, is important in the pathophysiology of chytridiomycosis. Amphibian plasma potassium concentrations are maintained at constant levels across seasons (27), and even moderate hypokalemia is dangerous in humans (28).

Our results support the epidermal dysfunction hypothesis, which suggests that *Bd* disrupts cutaneous osmoregulatory function, leading to electrolyte imbalance and death. The ability of *Bd* to

compromise the epidermis explains how a superficial skin fungus can be fatal to many species of amphibians; their existence depends on the physiological interactions of the skin with the external environment (16–19). Disease outbreaks capable of causing population declines require the alignment of multiple variables, including a life-compromising pathophysiology (1). Resolving the pathogenesis of chytridiomycosis is a key step in understanding this unparalleled pandemic.

References and Notes

1. P. Daszak, A. A. Cunningham, A. D. Hyatt, *Divers. Distrib.* **9**, 141 (2003).
2. F. de Castro, B. Bolker, *Ecol. Lett.* **8**, 117 (2005).
3. L. Berger *et al.*, *Proc. Natl. Acad. Sci. U.S.A.* **95**, 9031 (1998).
4. D. B. Wake, V. T. Vredenburg, *Proc. Natl. Acad. Sci. U.S.A.* **105**, 11466 (2008).
5. H. McCallum, *Conserv. Biol.* **19**, 1421 (2005).
6. K. R. Lips *et al.*, *Proc. Natl. Acad. Sci. U.S.A.* **103**, 3165 (2006).
7. L. F. Skerratt *et al.*, *EcoHealth* **4**, 125 (2007).
8. L. M. Schloegel *et al.*, *EcoHealth* **3**, 35 (2006).
9. D. C. Woodhams, R. A. Alford, *Conserv. Biol.* **19**, 1449 (2005).
10. K. M. Mitchell, T. S. Churcher, T. W. J. Garner, M. C. Fisher, *Proc. R. Soc. London Ser. B* **275**, 329 (2008).
11. M. Schaechter, B. I. Eisensteing, G. Medoff, in *Mechanisms of Microbial Disease* (Williams & Wilkins, Baltimore, 1998), pp. 419–439.
12. J. E. Longcore, A. P. Pessier, D. K. Nichols, *Mycologia* **91**, 219 (1999).
13. L. Berger *et al.*, *Dis. Aquat. Organ.* **68**, 65 (2005).
14. D. C. Woodhams *et al.*, *Anim. Conserv.* **10**, 409 (2007).
15. E. B. Rosenblum, J. E. Stajick, N. Maddox, M. B. Eisen, *Proc. Natl. Acad. Sci. U.S.A.* **105**, 17034 (2008).
16. H. Heatwole, in *Amphibian Biology, Vol. 1. The Integument*, H. Heatwole, G. T. Bartholomew, Eds. (Surrey Beatty, Chipping Norton, New South Wales, 1994), pp. 98–168.
17. R. G. Boutilier, D. F. Stiffler, D. P. Toews, in *Environmental Physiology of the Amphibians*, M. E. Feder, W. W. Burggren, Eds. (Univ. of Chicago Press, Chicago, 1992), pp. 81–124.

18. I. J. Deyrup, in *Physiology of the Amphibia*, J. A. Moore, Ed. (Academic Press, New York, 1964), vol. 1, pp. 251–315.
19. K. M. Wright, B. R. Whitaker, in *Amphibian Medicine and Captive Husbandry*, K. M. Wright, B. R. Whitaker, Eds. (Krieger, Malabar, FL, 2001), pp. 318–319.
20. J. Voyles *et al.*, *Dis. Aquat. Organ.* **77**, 113 (2007).
21. L. Berger, G. Marantelli, L. F. Skerratt, R. Speare, *Dis. Aquat. Organ.* **68**, 47 (2005).
22. D. J. Benos, L. J. Mandel, R. S. Balaban, *J. Gen. Physiol.* **73**, 307 (1979).
23. R. H. Alvarado, T. H. Dietz, T. L. Mullen, *Am. J. Physiol.* **229**, 869 (1975).
24. G. A. Castillo, G. G. Orce, *Comp. Biochem. Physiol. A* **118**, 1145 (1997).
25. N. A. Paradis, H. R. Halperin, R. M. Nowak, in *Cardiac Arrest: The Science and Practice of Resuscitation Medicine* (Williams & Wilkins, Baltimore, 1996), pp. 621–623.
26. See supporting material on Science Online.
27. D. R. Robertson, *Comp. Biochem. Physiol. A* **60**, 387 (1978).
28. F. J. Gennari, *N. Engl. J. Med.* **339**, 451 (1998).
29. We thank A. Hyatt and V. Olsen for assistance with PCR and S. Bell, J. Browne, S. Cashins, S. Garland, M. Holdsworth, C. Manicom, L. Owens, R. Puschendorf, K. Rose, E. Rosenblum, D. Rudd, A. Storfer, J. VanDerwal, B. Voyles, and J. Warner for project assistance and editing. Supported by Australian Research Council Discovery Project grant DP0452826, Australian Government Department of Environment and Heritage grant RFT 43/2004, and the Wildlife Preservation Society of Australia. Animals were collected with permission from Queensland Parks and Wildlife Service (scientific permits WISPO3866106 and WISPO4143907; movement permit WIWM04381507) and New South Wales Parks and Wildlife Service (import license IE0705693).

Supporting Online Material

www.sciencemag.org/cgi/content/full/326/5952/582/DC1
Materials and Methods

SOM Text

Figs. S1 and S2

Tables S1 and S2

References

26 May 2009; accepted 26 August 2009

10.1126/science.1176765

Detection of an Infectious Retrovirus, XMRV, in Blood Cells of Patients with Chronic Fatigue Syndrome

Vincent C. Lombardi,^{1*} Francis W. Ruscetti,^{2*} Jaydip Das Gupta,³ Max A. Pfost,¹ Kathryn S. Hagen,¹ Daniel L. Peterson,¹ Sandra K. Ruscetti,⁴ Rachel K. Bagni,⁵ Cari Petrow-Sadowski,⁶ Bert Gold,² Michael Dean,² Robert H. Silverman,³ Judy A. Mikovits^{1†}

Chronic fatigue syndrome (CFS) is a debilitating disease of unknown etiology that is estimated to affect 17 million people worldwide. Studying peripheral blood mononuclear cells (PBMCs) from CFS patients, we identified DNA from a human gammaretrovirus, xenotropic murine leukemia virus–related virus (XMRV), in 68 of 101 patients (67%) as compared to 8 of 218 (3.7%) healthy controls. Cell culture experiments revealed that patient-derived XMRV is infectious and that both cell-associated and cell-free transmission of the virus are possible. Secondary viral infections were established in uninfected primary lymphocytes and indicator cell lines after their exposure to activated PBMCs, B cells, T cells, or plasma derived from CFS patients. These findings raise the possibility that XMRV may be a contributing factor in the pathogenesis of CFS.

Chronic fatigue syndrome (CFS) is a disorder of unknown etiology that affects multiple organ systems in the body. Patients with CFS display abnormalities in immune sys-

tem function, often including chronic activation of the innate immune system and a deficiency in natural killer cell activity (1, 2). A number of viruses, including ubiquitous herpesviruses and

enteroviruses, have been implicated as possible environmental triggers of CFS (1). Patients with CFS often have active β herpesvirus infections, suggesting an underlying immune deficiency.

The recent discovery of a gammaretrovirus, xenotropic murine leukemia virus–related virus (XMRV), in the tumor tissue of a subset of prostate cancer patients prompted us to test whether XMRV might be associated with CFS. Both of these disorders, XMRV-positive prostate cancer and CFS, have been linked to alterations in the antiviral enzyme RNase L (3–5). Using the Whittemore Peterson Institute's (WPI's) national

¹Whittemore Peterson Institute, Reno, NV 89557, USA.

²Laboratory of Experimental Immunology, National Cancer Institute–Frederick, Frederick, MD 21701, USA. ³Department of Cancer Biology, The Lerner Research Institute, The Cleveland Clinic Foundation, Cleveland, OH 44195, USA.

⁴Laboratory of Cancer Prevention, National Cancer Institute–Frederick, Frederick, MD 21701, USA. ⁵Advanced Technology Program, National Cancer Institute–Frederick, Frederick, MD 21701, USA. ⁶Basic Research Program, Scientific Applications International Corporation, National Cancer Institute–Frederick, Frederick, MD 21701, USA.

*These authors contributed equally to this work.

†To whom correspondence should be addressed. E-mail: judym@wpinstitute.org

tissue repository, which contains samples from well-characterized cohorts of CFS patients, we isolated nucleic acids from PBMCs and assayed the samples for XMRV *gag* sequences by nested polymerase chain reaction (PCR) (5, 6). Of the 101 CFS samples analyzed, 68 (67%) contained XMRV *gag* sequence. Detection of XMRV was confirmed in 7 of 11 WPI CFS samples at the Cleveland Clinic by PCR-amplifying and sequencing segments of XMRV *env* [352 nucleotides (nt)] and *gag* (736 nt) in CFS PBMC DNA (Fig. 1A) (6). In contrast, XMRV *gag* sequences were detected in 8 of 218 (3.7%) PBMC DNA specimens from healthy individuals. Of the 11 healthy control DNA samples analyzed by PCR for both *env* and *gag*, only one sample was positive for *gag* and none for *env* (Fig. 1B). In all positive cases, the XMRV *gag* and *env* sequences were more than 99% similar to those previously reported for prostate tumor-associated strains of XMRV (VP62, VP35, and VP42) (fig. S1) (5).

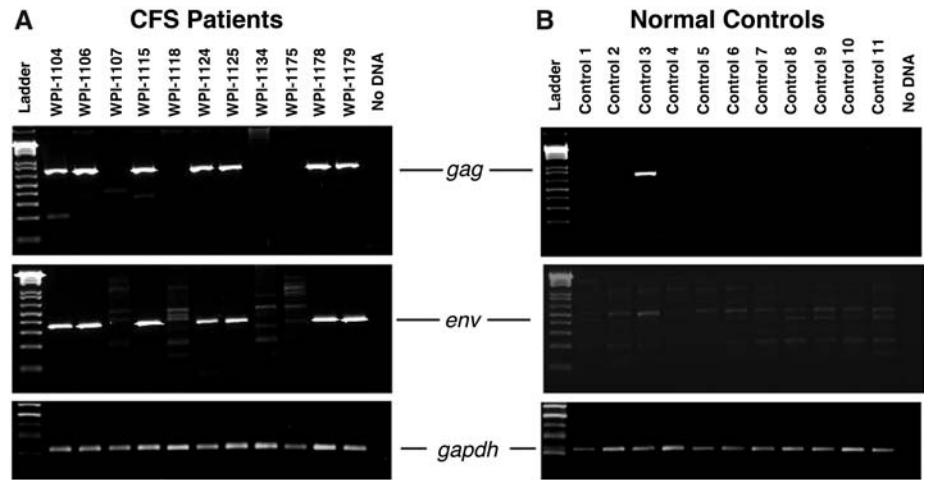


Fig. 1. XMRV sequences in PBMC DNA from CFS patients. Single-round PCR results for *gag*, *env*, and *gapdh* sequences in PBMCs of (A) CFS patients and (B) healthy controls are shown. The positions of the amplicons are indicated and DNA markers (ladder) are shown. These are representative results from one group of 20 patients.

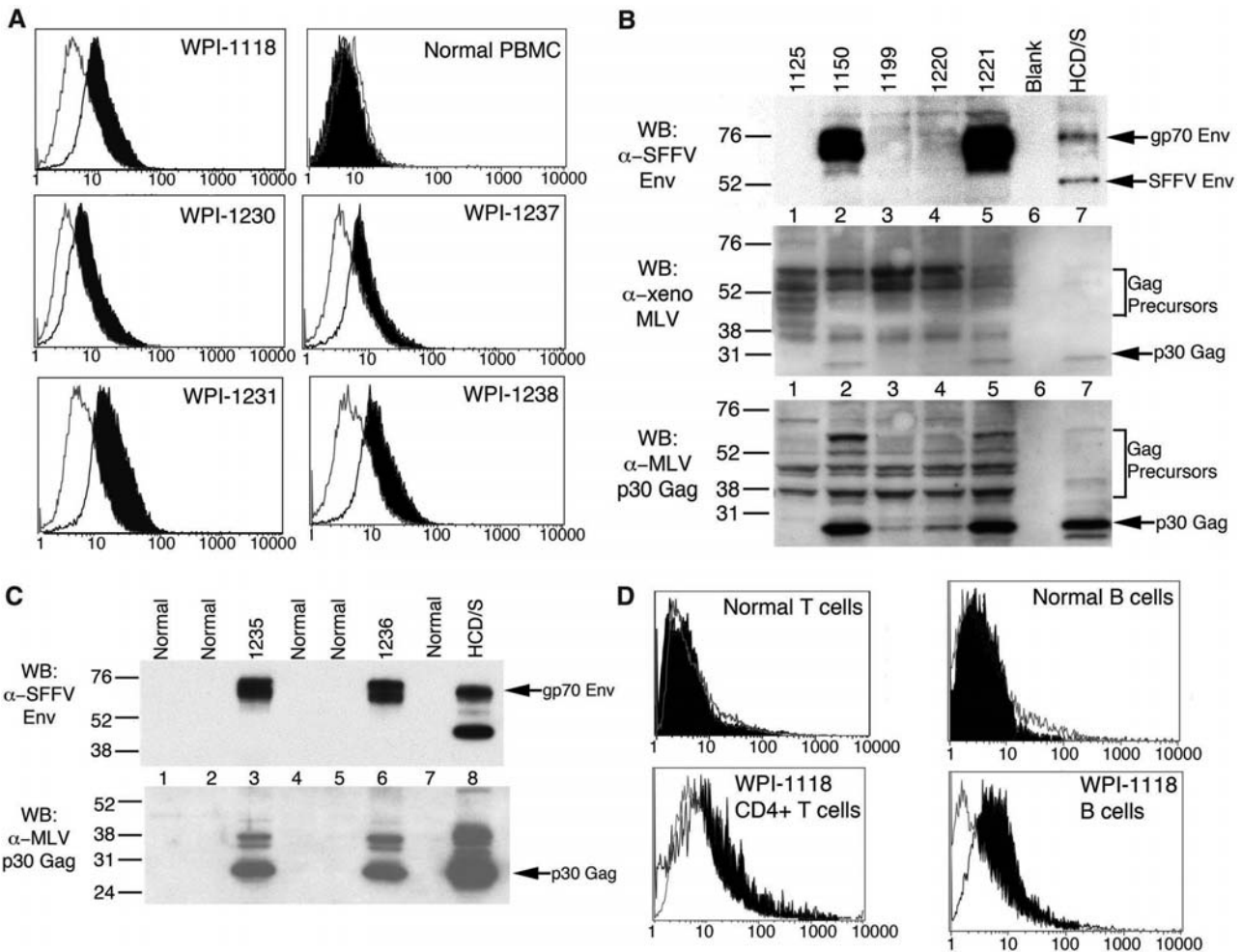


Fig. 2. Expression of XMRV proteins in PBMCs from CFS patients. (A) PBMCs were activated with phytohemagglutinin and interleukin-2, reacted with a mAb to MLV p30 Gag, and analyzed by IFC. (B) Lysates of activated PBMCs from CFS patients (lanes 1 to 5) were analyzed by Western blots with rat mAb to SFFV Env (top panel), goat antiserum to xenotopic MLV (middle panel), or goat antiserum to MLV p30 Gag (bottom panel). Lane 7, lysate from SFFV-infected HCD-57 cells. Molecular weight markers in kilodaltons are at left. (C) Lysates of activated PBMCs from healthy donors (lanes 1, 2, 4, 5, and 7) or from CFS patients (lanes 3 and 6) were analyzed by Western blots using rat mAb to SFFV Env (top panel) or goat antiserum to MLV p30 Gag (bottom panel). Lane 8, SFFV-infected HCD-57 cells. Molecular weight (MW) markers in kilodaltons are at left. (D) CD4⁺ T cells (left) or CD19⁺ B cells (right) were purified, activated, and examined by flow cytometry for XMRV Gag with a mAb to MLV p30 Gag.

Lysates of activated PBMCs from healthy donors (lanes 1, 2, 4, 5, and 7) or from CFS patients (lanes 3 and 6) were analyzed by Western blots using rat mAb to SFFV Env (top panel) or goat antiserum to MLV p30 Gag (bottom panel). Lane 8, SFFV-infected HCD-57 cells. Molecular weight (MW) markers in kilodaltons are at left. (D) CD4⁺ T cells (left) or CD19⁺ B cells (right) were purified, activated, and examined by flow cytometry for XMRV Gag with a mAb to MLV p30 Gag.

Sequences of full-length XMRV genomes from two CFS patients and a partial genome from a third patient were generated (table S1). CFS XMRV strains 1106 and 1178 each differed by 6 nt from

the reference prostate cancer strain XMRV VP62 (EF185282), and with the exception of 1 nt, the variant nucleotides mapped to different locations within the XMRV genome, suggesting indepen-

dent infections. In comparison, prostate cancer-derived XMRV strains VP35 and VP42 differed from VP62 by 13 and 10 nt, respectively. Thus, the complete XMRV genomes in these CFS patients

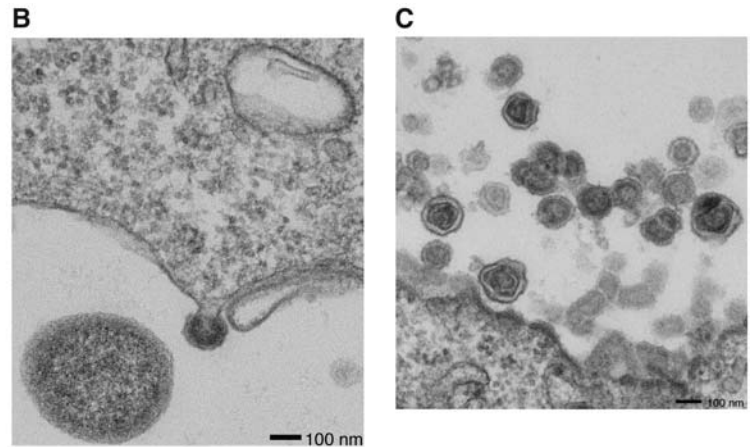
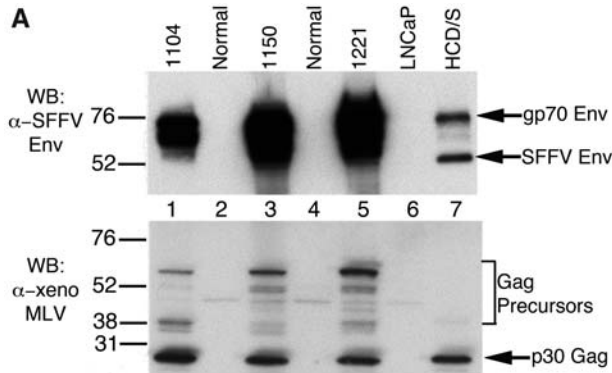
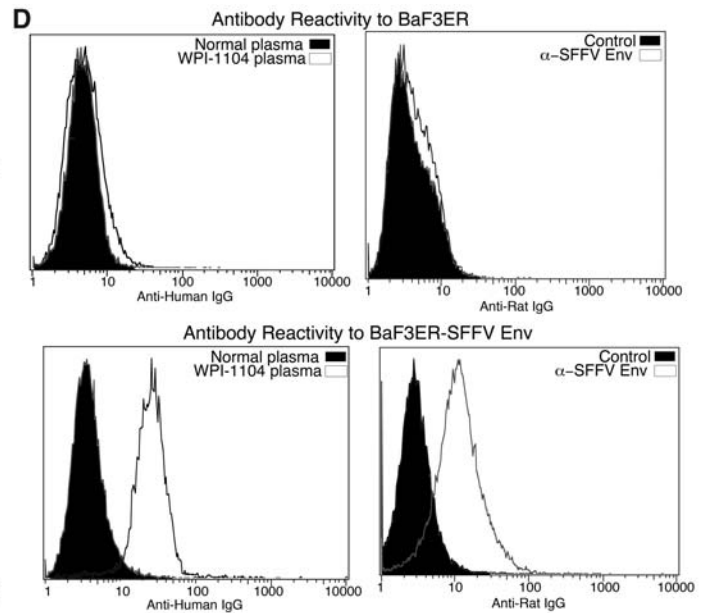
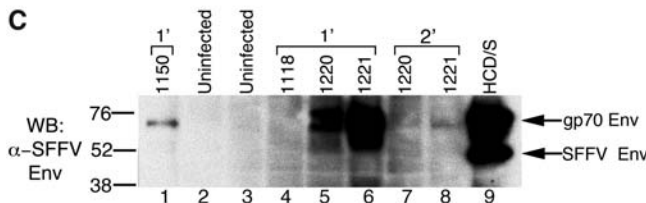
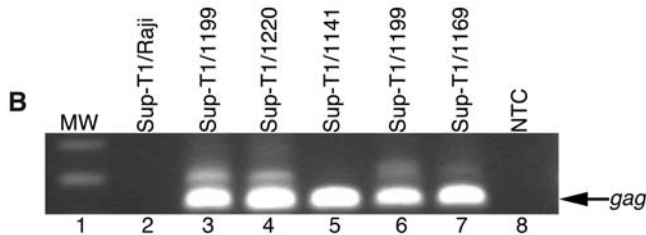
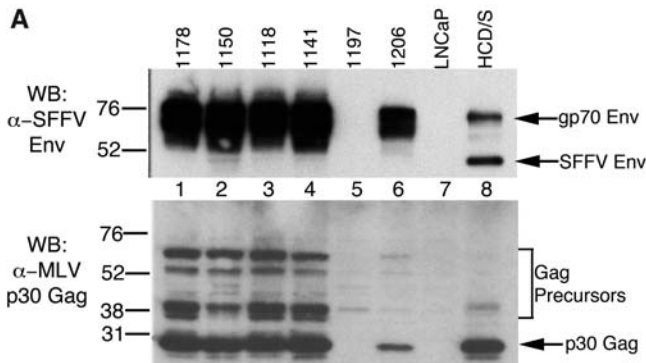


Fig. 3. Infectious XMRV in PBMCs from CFS patients. (A) Lysates of LNCaP cells cocultured with PBMCs from CFS patients (lanes 1, 3, and 5) or healthy donors (lanes 2 and 4) were analyzed by Western blots with rat mAb to SFFV Env (top panel) or goat antiserum to xenotropic MLV (bottom panel). Lane 6, uninfected LNCaP; lane 7,

SFFV-infected HCD-57 cells. MW markers in kilodaltons are at left. (B) Transmission electron micrograph of a budding viral particle from LNCaP cells infected by incubation with an activated T cell culture from a CFS patient. (C) Transmission electron micrograph of virus particles released by infected LNCaP cells.



Lane 8, no template control (NTC). (C) Normal T cells were exposed to cell-free supernatants obtained from T cells (lanes 1, 5, and 6) or B cells (lane 4) from CFS patients. Lanes 7 and 8 are secondary infections of normal activated T cells. Initially, uninfected primary T cells were exposed to supernatants from PBMCs of patients WPI-1220 (lane 7) and WPI-1221 (lane 8). Lanes 2 and 3, uninfected T cells; lane 9, SFFV-infected HCD-57 cells. Viral protein expression was detected by Western blot with a rat mAb to SFFV Env. MW markers in kilodaltons are at left. (D) Plasma samples from a CFS patient or from a healthy control as well as SFFV Env mAb or control were reacted with BaF3ER cells (top) or BaF3ER cells expressing recombinant SFFV Env (bottom) and analyzed by flow cytometry. IgG, immunoglobulin G.

Fig. 4. Infectious XMRV and antibodies to XMRV in CFS patient plasma. (A) Plasma from CFS patients (lanes 1 to 6) were incubated with LNCaP cells and lysates were prepared after six passages. Viral protein expression was detected by Western blots with rat mAb to SFFV Env (top panel) or goat antiserum to MLV p30 Gag (bottom panel). Lane 7, uninfected LNCaP; lane 8, SFFV-infected HCD-57 cells. MW markers in kilodaltons are at left. (B) Cell-free transmission of XMRV to the SupT1 cell line was demonstrated using transwell coculture with patient PBMCs, followed by nested *gag* PCR. Lane 1, MW marker. Lane 2, SupT1 cocultured with Raji. Lanes 3 to 7, SupT1 cocultured with CFS patient PBMCs. Lane 8, no template control (NTC). (C) Normal T cells were exposed to cell-free supernatants obtained from T cells (lanes 1, 5, and 6) or B cells (lane 4) from CFS patients. Lanes 7 and 8 are secondary infections of normal activated T cells. Initially, uninfected primary T cells were exposed to supernatants from PBMCs of patients WPI-1220 (lane 7) and WPI-1221 (lane 8). Lanes 2 and 3, uninfected T cells; lane 9, SFFV-infected HCD-57 cells. Viral protein expression was detected by Western blot with a rat mAb to SFFV Env. MW markers in kilodaltons are at left. (D) Plasma samples from a CFS patient or from a healthy control as well as SFFV Env mAb or control were reacted with BaF3ER cells (top) or BaF3ER cells expressing recombinant SFFV Env (bottom) and analyzed by flow cytometry. IgG, immunoglobulin G.

were >99% identical in sequence to those detected in patients with prostate cancer. To exclude the possibility that we were detecting a murine leukemia virus (MLV) laboratory contaminant, we determined the phylogenetic relationship among endogenous (non-ecotropic) MLV sequences, XMRV sequences, and sequences from CFS patients 1104, 1106, and 1178 (fig. S2). XMRV sequences from the CFS patients clustered with the XMRV sequences from prostate cancer cases and formed a branch distinct from non-ecotropic MLVs common in inbred mouse strains. Thus, the virus detected in the CFS patients' blood samples is unlikely to be a contaminant.

To determine whether XMRV proteins were expressed in PBMCs from CFS patients, we developed intracellular flow cytometry (IFC) and Western blot assays, using antibodies (Abs) with novel viral specificities. These antibodies included, among others, (i) rat monoclonal antibody (mAb) to the spleen focus-forming virus (SFFV) envelope (Env), which reacts with all polytropic and xenotropic MLVs (7); (ii) goat antisera to whole mouse NZB xenotropic MLV; and (iii) a rat mAb to MLV p30 Gag (8). All of these Abs detected the human VP62 XMRV strain grown in human Raji, LNCaP, and Sup-T1 cells (fig. S3) (5). IFC of activated lymphocytes (6, 9) revealed that 19 of 30 PBMC samples from CFS patients reacted with the mAb to MLV p30 Gag (Fig. 2A). The majority of the 19 positive samples also reacted with antisera to other purified MLV proteins (fig. S4A). In contrast, 16 healthy control PBMC cultures tested negative (Fig. 2A and fig. S4A). These results were confirmed by Western blots (Fig. 2, B and C) (6) using Abs to SFFV Env, mouse xenotropic MLV, and MLV p30 Gag. Samples from five healthy donors exhibited no expression of XMRV proteins (Fig. 2C). The frequencies of CFS cases versus healthy controls that were positive and negative for XMRV sequences were used to calculate a Pearson χ^2 value of 154 (two-tailed *P* value of 8.1×10^{-35}). These data yield an odds ratio of 54.1 (a 95% confidence interval of 23.8 to 122), suggesting a nonrandom association with XMRV and CFS patients.

To determine which types of lymphocytes in blood express XMRV, we isolated B and T cells from one patient's PBMCs (6). Using mAb to MLV p30 Gag and IFC, we found that both activated T and B cells were infected with XMRV (Fig. 2D and fig. S4A). Furthermore, using mAb to SFFV Env, we found that >95% of the cells in a B cell line developed from another patient were positive for XMRV Env (fig. S4B). XMRV protein expression in CFS patient-derived activated T and B cells grown for 42 days in culture was confirmed by Western blots (fig. S4C) using Abs to SFFV Env and xenotropic MLV.

We next investigated whether the viral proteins detected in PBMCs from CFS patients represent infectious XMRV. Activated lymphocytes (6) were cocultured with LNCaP, a prostate cancer cell line with defects in both the JAK-STAT and RNase L pathways (10, 11) that was previ-

ously shown to be permissive for XMRV infection (12). After coculture with activated PBMCs from CFS patients, LNCaP cells expressed XMRV Env and multiple XMRV Gag proteins when analyzed by Western blot (Fig. 3A) and IFC (fig. S5A). Transmission electron microscopy (EM) of the infected LNCaP cells (Fig. 3B), as well as virus preparations from these cells (Fig. 3C), revealed 90- to 100-nm-diameter budding particles consistent with a gamma (type C) retrovirus (13).

We also found that XMRV could be transmitted from CFS patient plasma to LNCaP cells when we applied a virus centrifugation protocol to enhance infectivity (6, 14, 15). Both XMRV gp70 Env and p30 Gag were abundantly expressed in LNCaP cells incubated with plasma samples from 10 of 12 CFS patients, whereas no viral protein expression was detected in LNCaP cells incubated with plasma samples from 12 healthy donors (Fig. 4A). Likewise, LNCaP cells incubated with patient plasma tested positive for XMRV p30 Gag in IFC assays (fig. S5B). We also observed cell-free transmission of XMRV from the PBMCs of CFS patients to the T cell line SupT1 (Fig. 4B) and both primary and secondary transmission of cell-free virus from the activated T cells of CFS patients to normal T cell cultures (Fig. 4C). Together, these results suggest that both cell-associated and cell-free transmission of CFS-associated XMRV are possible.

We next investigated whether XMRV stimulates an immune response in CFS patients. For this purpose, we developed a flow cytometry assay that allowed us to detect Abs to XMRV Env by exploiting its close homology to SFFV Env (16). Plasma from 9 out of 18 CFS patients infected with XMRV reacted with a mouse B cell line expressing recombinant SFFV Env (BaF3ER-SFFV-Env) but not to SFFV Env negative control cells (BaF3ER), analogous to the binding of the SFFV Env mAb to these cells (Fig. 4D and S6A). In contrast, plasma from seven healthy donors did not react (Fig. 4D and fig. S6A). Furthermore, all nine positive plasma samples from CFS patients but none of the plasma samples from healthy donors blocked the binding of the SFFV Env mAb to SFFV Env on the cell surface (fig. S6B). These results are consistent with the hypothesis that CFS patients mount a specific immune response to XMRV.

Neurological maladies and immune dysfunction with inflammatory cytokine and chemokine up-regulation are some of the most commonly reported features associated with CFS. Several retroviruses, including the MLVs and the primate retroviruses HIV and HTLV-1, are associated with neurological diseases as well as cancer (17). Studies of retrovirus-induced neurodegeneration in rodent models have indicated that vascular and inflammatory changes mediated by cytokines and chemokines precede the neurological pathology (18, 19). The presence of infectious XMRV in lymphocytes may account for some of these observations of altered immune responsiveness and neurological function in CFS patients.

We have discovered a highly significant association between the XMRV retrovirus and CFS. This observation raises several important questions. Is XMRV infection a causal factor in the pathogenesis of CFS or a passenger virus in the immunosuppressed CFS patient population? What is the relationship between XMRV infection status and the presence or absence of other viruses that are often associated with CFS (e.g., herpesviruses)? Conceivably these viruses could be cofactors in pathogenesis, as is the case for HIV-mediated disease, in which co-infecting pathogens play an important role (20). Patients with CFS have an elevated incidence of cancer (21). Does XMRV infection alter the risk of cancer development in CFS? As noted above, XMRV has been detected in prostate tumors from patients expressing a specific genetic variant of the *RNASEL* gene (5). In contrast, in our study of this CFS cohort, we found that XMRV infection status does not correlate with the *RNASEL* genotype (6) (table S2).

Finally, it is worth noting that 3.7% of the healthy donors in our study tested positive for XMRV sequences. This suggests that several million Americans may be infected with a retrovirus of as yet unknown pathogenic potential.

References and Notes

1. L. D. Devanur, J. R. Kerr, *J. Clin. Virol.* **37**, 139 (2006).
2. T. L. Whiteside, D. Friberg, *Am. J. Med.* **105**, 275 (1998).
3. R. J. Suhadolnik et al., *J. Interferon Cytokine Res.* **17**, 377 (1997).
4. G. Casey et al., *Nat. Genet.* **32**, 581 (2002).
5. A. Urisman et al., *PLoS Pathog.* **2**, e25 (2006).
6. Materials and methods are available as supporting material on Science Online.
7. R. Wolff, S. Koller, J. Ruscetti, *Virology* **43**, 472 (1982).
8. B. Chesebro et al., *Virology* **127**, 134 (1983).
9. K. A. Smith, F. W. Ruscetti, *Adv. Immunol.* **31**, 137 (1981).
10. G. Dunn, K. Sheehan, L. Old, R. Schreiber, *Cancer Res.* **65**, 3447 (2005).
11. Y. Xiang et al., *Cancer Res.* **63**, 6795 (2003).
12. B. Dong et al., *Proc. Natl. Acad. Sci. U.S.A.* **104**, 1655 (2007).
13. B. J. Poiesz et al., *Proc. Natl. Acad. Sci. U.S.A.* **77**, 7415 (1980).
14. G. R. Pietroboni, G. B. Harnett, M. R. Bucens, *J. Virol. Methods* **24**, 85 (1989).
15. S. M. Yoo et al., *J. Virol. Methods* **154**, 160 (2008).
16. L. Wolff, E. Scolnick, S. Ruscetti, *Proc. Natl. Acad. Sci. U.S.A.* **80**, 4718 (1983).
17. C. Power, *Trends Neurosci.* **24**, 162 (2001).
18. X. Li, C. Hanson, J. Cmarik, S. Ruscetti, *J. Virol.* **83**, 4912 (2009).
19. K. E. Peterson, B. Chesebro, *Curr. Top. Microbiol. Immunol.* **303**, 67 (2006).
20. A. Lisco, C. Vanpouille, L. Margolis, *Curr. HIV/AIDS Rep.* **6**, 5 (2009).
21. P. H. Levine et al., *Cancer Res.* **52**, 5516s (1992).
22. We thank D. Bertolette, Y. Huang, C. Hanson, and J. Troxler for technical assistance; K. Nagashima for EM; and C. Ware and K. Hunter for discussions. Funded by the Whittemore Peterson Institute and the Whittemore Family Foundation; the National Cancer Institute (NCI); NIH (under contract HHSN26120080001E); and grants to R.H.S. from NCI/NIH (CA104943), the U.S. DoD Prostate Cancer Research Program (W81XWH-07-1338), the V Foundation for Cancer Research, the Charlotte Geyer Foundation, and Mal and Lea Bank. The content of this publication does not reflect the views or policies of the U.S. DHHS, nor does mention of trade names, commercial products, or organizations imply endorsement by the U.S. government.

R.H.S. may receive royalty payments in the future from Abbott Laboratories. GenBank accession numbers are as follows: WPI-1130, GQ483508; WPI-1138, GQ483509; WPI-1169, GQ483510; WPI-1178, GQ497343; WPI-1106, GQ497344; and WPI-1104, GQ497345.

Note added in proof: V.C.L. is operations manager of Viral Immune Pathologies Laboratory, which is in negotiations

with the Whittemore Peterson Institute to offer a diagnostic test for XMRV.

Supporting Online Material

www.sciencemag.org/cgi/content/full/1179052/DC1
Materials and Methods
Figs. S1 to S6

Tables S1 and S2
References

7 May 2009; accepted 31 August 2009
Published online 8 October 2009;
10.1126/science.1179052
Include this information when citing this paper.

Complete Reconstitution of a Highly Reducing Iterative Polyketide Synthase

Suzanne M. Ma,¹ Jesse W.-H. Li,² Jin W. Choi,³ Hui Zhou,¹ K. K. Michael Lee,³ Vijayalakshmi A. Moorthie,² Xinkai Xie,¹ James T. Kealey,⁴ Nancy A. Da Silva,³ John C. Vederas,^{2*} Yi Tang^{1*}

Highly reducing iterative polyketide synthases are large, multifunctional enzymes that make important metabolites in fungi, such as lovastatin, a cholesterol-lowering drug from *Aspergillus terreus*. We report efficient expression of the lovastatin nonaketide synthase (LovB) from an engineered strain of *Saccharomyces cerevisiae*, as well as complete reconstitution of its catalytic function in the presence and absence of cofactors (the reduced form of nicotinamide adenine dinucleotide phosphate and *S*-adenosylmethionine) and its partner enzyme, the enoyl reductase LovC. Our results demonstrate that LovB retains correct intermediates until completion of synthesis of dihydromonacolin L, but off-loads incorrectly processed compounds as pyrones or hydrolytic products. Experiments replacing LovC with analogous MlcG from compactin biosynthesis demonstrate a gate-keeping function for this partner enzyme. This study represents a key step in the understanding of the functions and structures of this family of enzymes.

Nature uses an amazing array of enzymes to make natural products (1). Among these metabolites, polyketides represent a class of over 7000 known structures of which more than 20 are commercial drugs (2). Among the most interesting but least understood enzymes making these compounds are the highly reducing iterative polyketide synthases (HR-IPKSs) found in filamentous fungi (3). In contrast to the well-studied bacterial type I PKSs that operate in an assembly line fashion (4), HR-IPKSs are megasynthases that function iteratively by using a set of catalytic domains repeatedly in different combinations to produce structurally diverse fungal metabolites (5). One such metabolite is lovastatin, a cholesterol-lowering drug from *Aspergillus terreus* (6). This compound is a precursor to simvastatin (Zocor, Merck, Whitehouse Station, NJ), a semi-synthetic drug that had annual sales of more than \$4 billion before loss of patent protection in 2006 (7).

Biosynthesis of lovastatin proceeds via dihydromonacolin L (acid form 1, lactone form 2), a product made by the HR-IPKS lovastatin nonaketide synthase (LovB), with the assistance of a separate enoyl reductase, LovC (8) (Fig. 1). LovB is a 335-kD protein that contains single copies of

ketosynthase (KS), malonyl-coenzyme A (CoA) acyltransferase (MAT), dehydratase (DH), methyltransferase (MT), ketoreductase (KR), and acyl-carrier protein (ACP) domains, as well as a section that is homologous to the condensation (CON) domain found in nonribosomal peptide synthetases (NRPSs) (9). It also contains a domain that resembles an enoyl reductase (ER) but lacks that activity. LovB must catalyze ~35 reactions and use different permutations of tailoring domains after each of the eight chain-extension steps to yield the nonaketide, dihydromonacolin L (2). This enzyme also catalyzes a biological Diels-Alder reaction during the assembly process to form the decalin ring system (10). In vitro studies of LovB (11) have been hampered by an inability to obtain sufficient amounts of the functional purified megasynthase from either *A. terreus* or heterologous *Aspergillus* hosts. As a result, the programming that governs metabolite assembly by LovB or other HR-IPKSs is not understood. Key aspects that remain to be elucidated include (i) the catalytic and structural roles of each domain in the megasynthase, (ii) substrate specificities of the catalytic domains and their tolerance to perturbation in megasynthase functions, and (iii) factors governing the choice of different combinations of domains during each iteration of catalysis. To initiate such studies, we engineered an expression system in yeast to produce large amounts of LovB and examined the influence of cofactors and the ER partner (e.g., LovC) on product formation.

The engineered *Saccharomyces cerevisiae* strain BJ5464-NpgA, which contains a chromo-

somal copy of the *Aspergillus nidulans* phosphopantetheinyl (ppant) transferase gene *npgA* (12), was the expression host. A C-terminal hexahistidine-tagged LovB was placed under the control of the *S. cerevisiae* *ADH2* promoter (13, 14) on an episomal plasmid (YEpLovB-6His). Abundant amounts of the intact LovB could be purified from the soluble fraction to near homogeneity with a final yield of ~4.5 mg/L (fig. S1). We used mass analysis of tryptic digest fragments to verify the identity of the recombinant LovB. The ACP domain of LovB was determined to be nearly completely phosphopantetheinylated by using a ppant ejection assay with high-resolution quadrupole orthogonal acceleration-time-of-flight mass spectrometry (fig. S2). To ascertain activity of the resulting LovB and to examine the necessity for cofactors, malonyl-CoA alone was first added to the purified enzyme in buffer. Whole-cell feeding studies of doubly [¹³C, ²H]-labeled acetate to cultures of *A. terreus* showed that all three acetate hydrogens were incorporated into the acetate-derived starter units for both the nonaketide and diketide moieties in lovastatin (15). The purified LovB can use malonyl-CoA for both chain priming and chain elongation, loading malonate with decarboxylation to make the acetyl starter unit. Although LovB is able to prime with and elongate the chain by two further condensations with malonyl-CoA, in the absence of the reduced form of nicotinamide adenine dinucleotide phosphate (NADPH), no ketoreduction occurs. The dominant product is lactone 3 (Fig. 2A, trace i), which forms by enolization and cyclization with off-loading of the unreduced triketide. Addition of NADPH to this system enables function of the KR domain. In this and subsequent experiments, the malonyl-CoA could be conveniently synthesized in situ by malonyl-CoA synthase (MatB) from *Rhizobium trifolii* using free malonate and CoA (16). With KR enabled, LovB makes penta-, hexa-, and heptaketide pyrones 4 to 6, as well as ketones 7 and 8 (Fig. 2A, trace ii). The structures were confirmed by chemical synthesis of authentic standards, except for heptaketide 6, which proved very unstable. However, the mass increase of 26 atomic mass units for 6 and its red shift in the ultraviolet spectrum when compared to 5 are consistent with its proposed heptaketide pyrone structure (table S3). Compounds 7 and 8 result from thioester hydrolysis of penta- and hexaketides stalling on the ACP at the β -keto stage. The resulting β -keto acids spontaneously decarboxylate to afford 7 and 8. Formation of compounds 4 to 8 illustrates that derailment in the normal programmed steps, namely the lack of methylation due to the absence of *S*-adenosylmethionine

¹Department of Chemical and Biomolecular Engineering, University of California, Los Angeles, CA 90095, USA.

²Department of Chemistry, University of Alberta, Edmonton, Alberta, T6G 2G2, Canada. ³Department of Chemical Engineering and Materials Science, University of California, Irvine, CA 92697, USA. ⁴Amryis Biotechnologies, 5885 Hollis Street, Suite 100, Emeryville, CA 94608, USA.

*To whom correspondence should be addressed. E-mail: john.vederas@ualberta.ca (J.C.V.); yitang@ucla.edu (Y.T.)